

Nanoparticles for super-resolution microscopy and single-molecule tracking

Dayong Jin^{1*}, Peng Xi^{2*}, Baoming Wang¹, Le Zhang¹, Jörg Enderlein^{3*} and Antoine M. van Oijen^{4*}

We review the use of luminescent nanoparticles in super-resolution imaging and single-molecule tracking, and showcase novel approaches to super-resolution imaging that leverage the brightness, stability, and unique optical-switching properties of these nanoparticles. We also discuss the challenges associated with their use in biological systems, including intracellular delivery and molecular targeting. In doing so, we hope to provide practical guidance for biologists and continue to bridge the fields of super-resolution imaging and nanoparticle engineering to support their mutual advancement.

Fluorescent proteins and organic dyes are commonly used as imaging probes in microscopy because of their small size and compatibility with biological samples. The advent of super-resolution microscopy made it possible to resolve cellular structures and subcellular organelles on the nanometer scale, and has revolutionized optical microscopy in the life sciences. However, for long-term tracking of single molecules and real-time super-resolution imaging of subcellular structures, brighter and more photostable probes are still needed to reveal the inner workings of the cell, as the current molecular dyes and fluorescent proteins are often too dim, can be optically switched in only a limited number of ways, and undergo rapid photobleaching.

Advances in the materials sciences have provided considerable opportunities to address the shortcomings of fluorescent dyes. Recent developments in the tailored design of nanoscopically sized probes with well-defined optical properties have resulted in a large collection of luminescent nanoparticles (Fig. 1) such as semiconductor quantum dots (QDots), upconversion nanocrystals (UCNPs), polymer dots (PDots), fluorescent nanodiamonds (FNDs), carbon-based nanodots (CDots), and nonfluorescent surface-enhanced Raman scattering (SERS) nanoparticles. Though they are still large compared with dye molecules (Fig. 1a) and substantial challenges lie ahead with respect to their complicated surface biochemistry, the many advantages of these nanoparticles have been successfully demonstrated and have started to pave the way for the cell biology and materials science communities to explore their full capability in subcellular functional imaging at the nanoscale. This Perspective focuses on the recent progress and future potential of these small luminescent nanoparticles for use in tracking single molecules and super-resolution imaging of subcellular structures.

Nanoparticles in super-resolution microscopy

QDots represent the first generation of inorganic fluorescent nanoparticles used for fluorescent labeling. Compared with conventional dyes, they have a much larger absorption coefficient, a higher luminescent quantum yield, and, as a result, greater brightness. QDots exhibit narrow-band emission (spectral width < 50 nm), and their emission color can be tuned through adjustments to their size (quantum confinement effect), which makes these particles ideal

for multicolor imaging applications¹ and a range of super-resolution imaging modes (Fig. 1b–f).

The commercially available ZnS-coated CdSe QDot 705 (from Thermo Fisher), CdTe QDot 700 nm, and CdTe QDot 720 nm (from PlasmaChem GmbH) have proven suitable for stimulated emission depletion (STED) microscopy with spatial resolutions in the range of 50 nm for single QDots, 85 nm for QDot-705-stained microtubule networks in HeLa cells², and 106 nm for vimentin filaments in fibroblasts³. The high stability of QDots allows for extended time-lapse imaging without any photophysical or photochemical processes that would diminish their brightness.

QDots have widespread applications in super-resolution optical fluctuation imaging (SOFI)⁴, and multicolor QDots (QDot 525, QDot 625, and QDot 705) have recently been used to achieve higher labeling densities to improve both temporal and spatial resolution⁵. New developments in material engineering have dramatically sped up the kinetics of QDot blinking to facilitate real-time optical microscopy with SOFI, thus enabling the use of spinning-disk confocal microscopy in association with bleaching/blinking-assisted localization microscopy and SOFI to obtain 3D super-resolution images⁶.

UCNPs represent an entirely new class of multiphoton probes that rely on high densities of multiphoton emitters in small particles⁷. Each particle contains thousands of codoped lanthanide ions that form a network of photon sensitizers and activators, which upconvert near-infrared photons into visible and ultraviolet ones. The large anti-Stokes spectral separation between excitation and emission renders these probes highly useful in background-free and photostable bioimaging^{8,9}.

Recent studies^{10,11} reported that thousands of emitters per nanoparticle can be activated by microscopes, resulting in a brightness that makes UCNPs suitable as single-molecule probes. Highly doped UCNPs were found to easily facilitate an optical population inversion at their intermediate metastable levels¹². As a result, a low saturation intensity of ~0.19 MW cm⁻² in upconversion STED microscopy was recorded, with a maximum resolution of 28 nm ($\lambda/36$) for optical imaging of single 13-nm UCNPs. High-speed (100- μ s dwelling time) super-resolution imaging of cellular cytoskeleton protein structures with a resolution of 80 nm has also been demonstrated¹³ (Fig. 1g).

¹Institute for Biomedical Materials & Devices (IBMD), Faculty of Science, University of Technology Sydney, Ultimo, NSW, Australia. ²Department of Biomedical Engineering, College of Engineering, Peking University, Beijing, China. ³Third Institute of Physics, University of Göttingen, Göttingen, Germany.

⁴School of Chemistry, University of Wollongong and Illawarra Health and Medical Research Institute, Wollongong, NSW, Australia.

*e-mail: dayong.jin@uts.edu.au; xipeng@pku.edu.cn; jenderl@gwdg.de; vanoijen@uow.edu.au

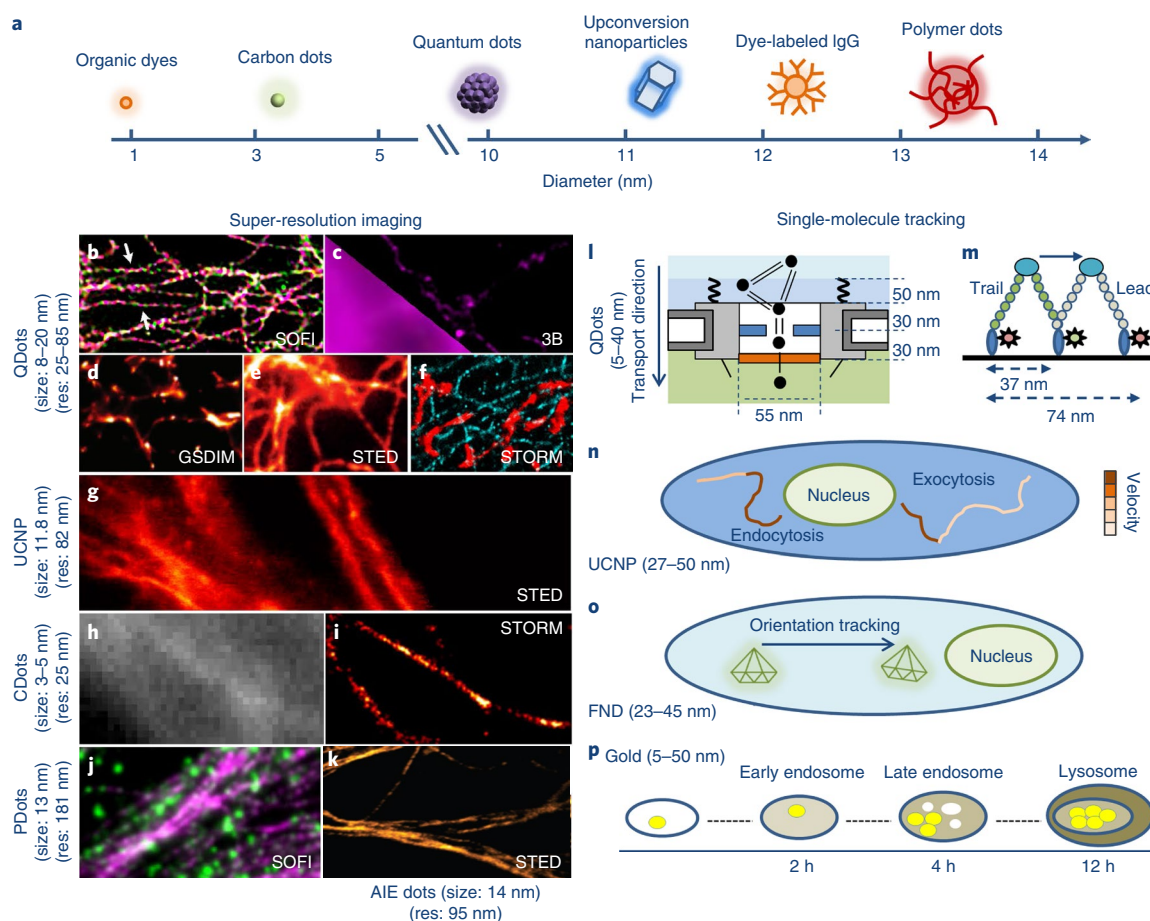


Fig. 1 | Luminescent nanoparticles used in super-resolution microscopy imaging and single-molecule tracking. **a**, Illustration of the physical dimensions of dye molecules, carbon dots, quantum dots, upconversion nanoparticles, dye-labeled IgG antibody, and polymer dots used in super-resolution microscopy. **b–f**, QDots used in super-resolution imaging. **b**, Multi-color SOFI image of microtubules in HeLa cells. **c**, 3B microscopy image of microtubules in HeLa cells. Reproduced with permission from ref. ². **d**, Ground-state depletion microscopy followed by individual molecule return (GSDIM) image of the microtubular network in mammalian PtK2 cells. Adapted with permission from ref. ⁷⁹. **e**, STED imaging of vimentin fibers in REF cells. **f**, Two-color STORM imaging of microtubules and mitochondria. Adapted with permission from ref. ⁸⁰. **g**, UCNPs used in STED imaging of microtubules in HeLa cells. **h,i**, CDots used in wide-field and STORM imaging of microtubules in HeLa cells. Adapted with permission from ref. ¹⁸. **j**, PDots used in multicolor SOFI microscopy imaging of microtubules in HeLa cells. Adapted with permission from ref. ⁸¹. **k**, AIE dots used in STED imaging of microtubules in HeLa cells. Adapted with permission from ref. ²¹. **l,m**, Single 5–40-nm QDots can be used to explore the mechanism of nanoparticle translocation through (l) the nuclear pore complex²⁴ and (m) a myosin motor²⁷. **n**, A schematic demonstrating the use of single 27–50-nm UCNPs³³ for intracellular single-nanoparticle tracking. **o**, A schematic illustrating the use of nanodiamonds for multidimensional tracking^{29,82}. **p**, A schematic illustrating the use of gold nanoparticles to quantify the processes of nanoparticle endocytosis and entrapment³⁵. Res, resolution.

Ultra-small CDots, 2–5 nm in diameter, have attracted substantial attention as subcellular targeting probes^{14,15}. They are highly stable in aqueous suspension and can be produced cost-effectively on a large scale. CDots have different functional groups such as –OH, –NH₂, and –COOH on the surface for further conjugation to biomolecules. Biocompatible CDots also exhibit emission blinking, and were found to be suitable for SOFI¹⁶ and STED microscopy¹⁵. In addition, CDots display photoswitching when used with an electron acceptor molecule, and were found to be suitable for single-molecule localization microscopy techniques like photoactivated localization microscopy (PALM) and stochastic optical reconstruction microscopy (STORM)¹⁷.

A type of 4.5-nm CDot has been developed with burst-like blinking behavior, and its use has been demonstrated for high-density specific labeling of a microtubule network¹⁸ (Fig. 1h,i). That work systematically compared the performance of CDots with that of Cy3, Cy5, Alexa Fluor 647, and CdSe/ZnS QDots 605, and concluded that CDots have improved brightness (8,000 photon counts per switching event) compared with

that of Cy3 (1,300–2,000 photon counts per switching event), great photostability (>30 min), and a very low duty cycle (0.003, versus 0.0003–0.0004 for Cy3), all of which make them highly suitable for STORM, with which the authors achieved a resolution of 25 nm. This technique allows super-resolution imaging of the clustering and distribution of membrane protein receptors.

PDots are particles that consist predominantly of π -conjugated polymers and have been shown to have superior brightness compared with that of conventional QDots¹⁹. Very small PDots (10 nm or less) were found to be suitable for fluctuation-based super-resolution techniques such as SOFI and 3B²⁰ (Fig. 1j). To functionalize the PDots, an optically inert polymer, poly(styrene-co-maleic anhydride) (PSMA), has been added. The PSMA polymer also generates surface carboxyl groups, which enables specific biomolecular conjugation through biotinylated antibodies²⁰. Their small size confers improved biocompatibility, and they were shown to be able to label a variety of subcellular organelles such as mitochondria, the nuclear envelope, and microtubules²⁰.

Another class of nanoparticles demonstrated for super-resolution imaging is aggregation-induced emission (AIE) dots²¹. These dots contain large numbers of chromophores within small particles (14 nm) that display strong fluorescence only when tightly packed in aggregates. These have been shown to be viable probes for specific subcellular labeling; recent work demonstrated the use of AIE dots in STED imaging of microtubule structures at 95-nm resolution^{21,22} (Fig. 1k).

Nanoparticles for single-molecule tracking

Figure 1l–p showcases intracellular tracking experiments using single luminescent nanoparticles. In contrast to the super-resolution imaging experiments described above, these types of single-molecule localization experiments do not rely on the characterization of structures with high label density, but instead are based on the tracking of a single particle through space and time with high precision. In live cell imaging, the insufficient brightness and photostability of organic dyes typically allow only 30-nm localization precision and trajectories composed of tens of scattered data points, whereas QDots and other inorganic nanoparticles allow precision below 5 nm at a temporal resolution of tens of milliseconds with thousands of data points. For example, with QDots, the diffusion dynamics of glycine receptors in the plasma membrane could be visualized easily for at least 20 min at a signal-to-noise ratio of about 50 (75-ms integration time)—almost an order of magnitude higher than the signal obtained with organic fluorophores. The lateral resolution reached 5–10 nm, well below the 40 nm achieved with the organic dye Cy3²³.

The ability to track single QDots has enabled scientists to study a range of intracellular transport processes. For instance, by conjugating single QDots with about 40 importin- β transport receptors each (resulting in a final hydrodynamic size of 30 ± 6 nm), researchers visualized the selectivity mechanism of the nuclear pore complex²⁴. This approach allowed detailed analysis of dozens of tracking trajectories, each containing hundreds of data points—statistics difficult to obtain via labeling with conventional dye molecules.

Real-time recording of the movement of endosomes containing nerve growth factor (NGF) conjugated to QDot 605 or QDot 705 revealed that a single NGF dimer may be sufficient to sustain signaling during retrograde axonal transport to the cell body²⁵. By showing that QDot labeling does not alter the trafficking and signaling of NGF, the study demonstrated that the use of QDots is a viable alternative to methods based on fluorescent dyes with much higher spatial and temporal resolution.

Ligand-conjugated QDots have been used to visualize binding to membrane receptors at the axon terminal and subsequent internalization of the QDot–ligand–receptor complex into an endosome, which in turn is retrogradely transported across the axons by dyneins. Under wide-field laser illumination, photo regeneration of reactive oxygen species by QDots was used to stochastically tether endosomes to microtubule-based structures in axons. By recording the movement of tethered endosomes at high frame rates (150 frames per second), the authors quantitatively verified the cooperative action of up to seven dyneins stochastically sharing the load²⁶.

The narrow emission spectra of streptavidin-functionalized QDots have allowed multicolor differential labeling and tracking of the individual heads of a single myosin V molecule motor. The use of QDots provided the high spatial and temporal resolution needed to show the alternating positions of each head in a hand-over-hand fashion as the myosin motor strode along actin²⁷.

The blinking of individual QDots has frequently been used to confirm the imaging of a single particle, but it also reduces the temporal resolution in continuous tracking experiments. A range of nonblinking nanoparticles, including PDots, nanodiamonds, and UCNPs that contain multiple emitters, have been developed for use in single-particle applications.

Single ~15-nm-diameter PDots have been used in 2D and 3D tracking experiments with a spatial localization precision of 1.4 nm at an acquisition rate of 50 frames per second²⁸. 3D single-molecule tracking has also been realized on a minute time scale with FNDs²⁹. Measurement of the changes in intraneuronal transport induced by brain-disease-related genetic risk factors was successfully achieved with FNDs³⁰. Using STED microscopy, scientists were able to distinguish single FNDs (~30 nm in diameter) in cells with a subdiffraction spatial resolution of approximately 40 nm³¹. UCNPs with a size of 50 nm have facilitated the long-term tracking of endocytosis and exocytosis for 24 h with 30-min intervals³² and the tracking of intracellular movement for 6 h in real time (20 frames per second) to visualize transport driven by molecular motors³³. Moreover, 3D tracking of UCNPs revealed intracellular diffusive motion and active transport processes³⁴. Nonfluorescent 50-nm gold nanoparticles coated with Cy3 dyes have been used to monitor the clustering behavior in intracellular transport through 2D real-time tracking³⁵. Single highly doped UCNPs are sufficiently bright to allow direct microscopic inspection and tracking by eye^{36,37}.

Luminescent nanoparticles, in particular hybrid nanoparticles with novel physical and biochemical properties, are extremely useful as self-correlative contrast agents in correlative microscopy³⁵. A particularly powerful example of such correlative microscopy is optical–electron microscopy, which integrates optical and electron microscopy to achieve higher spatial resolution^{23,25}.

The many applications highlighted here are testament to the catalytic effect that multidisciplinary approaches have on the development of smaller and brighter imaging probes, including their functionalization, conjugation, and delivery, and on the creation of new ways to illuminate subcellular structures and molecular interactions, which together are leading to the realization of nanoscale dynamic imaging studies.

Challenges

Even though a remarkable amount of progress has been made in the use of nanoparticles for super-resolution imaging and single-molecule tracking, there are still major limitations, such as the relatively large size of these nanoparticles and their complex surface chemistry, both of which give rise to difficulties in targeted intracellular delivery and specific labeling of subcellular targets. The interface chemistry and a variety of surface functionalization strategies have been reviewed elsewhere^{38,39}. Here we focus on potential solutions that might allow nanoparticles to become truly specific subcellular probes.

Delivering nanoparticles into live cells. Whereas organic dyes with specificity for cellular substructures, such as DAPI, Mitotracker, and LysoTracker, are small enough to permeate biological membranes of cells and organelles, the much larger size of nanoparticles typically requires processes such as receptor-mediated endocytosis for cellular uptake and intracellular delivery. As a result, extra steps are typically needed to enable nanoparticles to escape the endosomal/lysosomal environment and enter the cytoplasm to ultimately associate with their specific target structure.

Several physical methods have been developed to enable nanoparticles to enter the cytoplasm, including microinjection of nanoparticles directly into the cytoplasm with a fine-tipped microcapillary under a fluorescent microscope⁴⁰. Another method used for nanoparticle delivery is electroporation with an electric field pulse, which works by temporarily generating hydrophilic pores in the plasma membrane through which nanoparticles can pass. Although electroporation can be efficient, two associated drawbacks are aggregation of the nanoparticles and a high rate of cell mortality⁴¹. Finally, osmotic lysis has been used to release particles from the endosome. As an example, commercial QDot–streptavi-

din conjugates bound to biotinylated kinesins have been shown to migrate into the cytoplasm of cultured mammalian HeLa cells after osmotic lysis of pinocytic vesicles⁴². This loading method was not reported to cause visible alteration of the cell morphology, but it can be toxic to cells. Ideally, future methods will combine the benefits of these approaches to allow straightforward subcellular nanoparticle delivery and specific targeting.

Designing smaller nanoparticles. The design and synthesis of smaller and brighter luminescent nanoparticles for use in subcellular imaging applications continues to be a major goal. Smaller nanoparticles (ideally <5 nm in diameter) are preferred for biological applications because they are more stable, are less likely to sterically affect the function of their label target, and may move passively through the membranes of subcellular organelles. Conjugation of smaller nanoparticles with translocation peptides, dendrimers, and other pharmacophore ligands will confer further targeting specificity to nanoparticle probes.

Super-resolution microscopy requires nanoparticles to be smaller than the subcellular structures being imaged. A high labeling density is typically preferred, as according to the Nyquist–Shannon sampling theorem, the label density has to be high enough that the average distance between labels is two times smaller than the desired resolution. For example, for a resolution of 40 nm to be achieved, the average distance between two fluorescent dyes or nanoparticles has to be less than 20 nm. Figure 1 shows that the size ranges of nanoparticles used for successful super-resolution imaging experiments are much smaller than those of particles used for single-nanoparticle tracking.

It can be challenging to shrink nanoparticles without affecting their favorable properties. Generally speaking, the brightness of doped nanoparticles, such as UCNPs, PDots, and FNDs, decreases proportionally to the number of emitters they contain. Also, a smaller size increases the ratio of surface area to volume, thus leading to enhanced quenching and reduced brightness. Strategies such as optimization of crystal host and dopant concentrations and coating of nanocrystals with thin shells have been used to generate luminescent nanoparticles in the sub-10-nm range that maintain high brightness and optical stability.

A careful comparison of the brightness of single dye molecules, QDots, and PDots showed that the average intensity of a 10-nm Pdot inside cells was ~25 times brighter than that of a QDot 565 (15–20 nm) under the same conditions, and ~18 times brighter than an Alexa-Fluor-labeled antibody¹⁹. An IgG–Alexa Fluor 488 probe has a hydrodynamic diameter of 12 nm and contains an average of six dye molecules, but its brightness corresponds to that of only two to four dye molecules owing to self-quenching¹⁹. In a recent report, smaller PDots displayed decreased brightness compared with that of larger PDots, but still exhibited greater brightness than QDots. The brightness of 3-nm CDots has been reported as comparable to that of QDots¹⁶. Ideally, the nanoparticle probes to be developed should have both a small size and short conjugation linkers to keep the overall hydrodynamic diameter closer to the size of an IgG–dye probe (~12 nm).

Surface functionalization and bioconjugation. Surface functionalization and bioconjugation strategies determine the stability of nanoparticle probes in physiological environments and their specificity in labeling subcellular structures. For example, trivalent lanthanide-ion-doped UCNPs are less stable than PDots and CDots in physiological environments because of their highly positively charged surface, and therefore strategies should focus on using ligand molecules that provide more negative charges so as to form much stronger anchoring to UCNPs for efficient bioconjugation⁴³. Figure 2 surveys various approaches used in subcellular labeling and tracking experiments. Polymer (e.g., polyethylene glycol

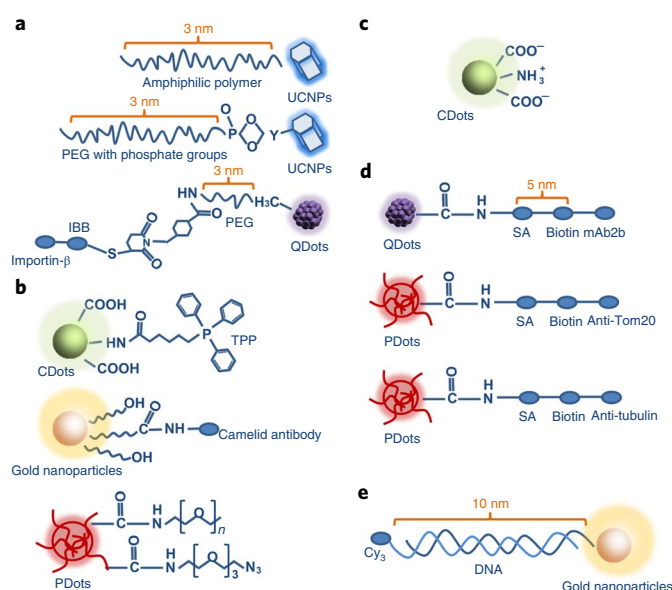


Fig. 2 | Surface functionalization and bioconjugation strategies for a range of nanoparticles used in subcellular staining and tracking applications.

a, Coating with a layer of PEG to minimize nonspecific binding^{24,33,37}. **b**, Selective conjugation of only a few functional groups to decrease the number of active binding sites and minimize aggregation and nonspecific binding^{14,83,84}. TPP, triphosphonium. **c**, Engineering of nanoparticles with zwitterionic surfaces to improve colloidal stability over a wide pH range and resistance to nonspecific protein adsorption⁴⁵. **d**, Conjugation to streptavidin (SA) with biotinylated antibodies^{20,23}. **e**, Coating with single-strand nucleotides to recognize and hybridize with complementary nucleotides³⁵.

(PEG)) coating of QDots and UCNPs has proven universally useful for minimizing nonspecific cellular uptake through endocytosis and attachment to the cell surface. Further, the high-molecular-weight polymer chains separate biomolecules from the nanoparticle surface to minimize undesired changes in biomolecular structure and/or functioning after coupling to the surface of nanoparticles^{24,33}. Biotinylated antibodies and streptavidin-coated nanoparticles are often used as adaptor molecules to improve the bioconjugation efficiency and simplicity between nanoparticle and antibody (Fig. 2d). For relatively large nanoparticles with large surface areas, reduction of the number of active binding sites helps to minimize aggregations and nonspecific binding caused by cross-linking with biomolecules⁴⁴.

Specific targeting of structures and proteins of interest is made possible by the functionalization of nanoparticles with specific recognition moieties, such as the nuclear-localization-sequence peptide²⁰, mitochondrial-localization-sequence peptide²⁰, glycine receptors²³, and neuron growth factors²⁵. PEG polymers have been used as linkers to functionalize nanoparticles with receptor-targeting moieties²⁴.

The surface charge of nanoparticles has also been identified as a critically important property for intracellular applications. Nanoparticles with zwitterionic surfaces show high colloidal stability over a wide pH range and high resistance to nonspecific protein adsorption⁴⁵. CDots with a passivating and zwitterionic ligand containing both carboxylic acid and amine moieties exhibited superior stability with a nearly neutral ζ potential at pH 7, and with a gradually increasing surface charge at decreasing pH. This property allowed cytoplasmic uptake and subsequent nuclear translocation of the CDots⁴⁵.

Table 1 | Comparison of the performance of tailored luminescent nanoparticles successfully used in subcellular super-resolution microscopy and/or single-nanoparticle tracking applications

	QDot ^{2,3,5,23,25,26,79,80,87-89}	FND ^{29-31,52}	UCNP ^{12,13,33,34,37}	PDot ^{19,20,28,81}	CDot ^{15,16,18}
Size (super-resolution) (nm)	8–20	35	11.8, 13	13	4.5
Size (tracking) (nm)	15–20	35–45	40	15	
Microscopy resolution (nm)	54 (STED) 85 (SOFI) 67 (3B) 45 (STORM)	29 (STED)	28 (STED) 82 (STED)	142 (SOFI)	25 (STORM) 30 (STED) 184 (SOFI)
Localization accuracy (nm)	10		4	1.4	
Brightness (tracking), measured by detected photon counts per step*	50–100 photons, 27 Hz	250 photons, 100 Hz	20,000 photons, 10 Hz	200,000 photons, 50 Hz	
STED saturation intensity (MW cm⁻²)	~60	0.82	0.19		
Fluorescence lifetime	8 ns	11.7 ns	~20 µs	1.5 ns	1.5–4 ns
Total tracking time	6 min, intermittency	20 min	6 h	3 s	
Laser wavelength (excitation/depletion) (nm)	628/775	532/740	980/808	405/488	405/592
Biological system studied (super-resolution imaging)	Microtubule		Microtubule	Microtubule, mitochondria, nuclear envelope	Microtubule, membrane protein receptors
Biological system studied (tracking)	Membrane protein, myosin motor, endosomes, selectivity mechanism of NPC	Live and fixed cells	Live cell	Fixed cell	
Multiplexing	Color	Limited	Color and lifetime	Color	Limited (by impurity)
Commercially available	Yes	Yes	Not yet	Not yet	Not yet
Bioconjugation for subcellular specific labeling	Relatively easy (well-developed labeling protocols)	Difficult (owing to relatively large size)	Relatively easy (tunable and uniform sizes, but highly charged surface)	Relatively easy (polymer surface)	Relatively easy (small size)

*The brightness of nanoparticles also depends on the excitation power used and the efficiency of detection in each particular experiment. NPC, nuclear pore complex.

One study found that charge and chemical surface groups have essential roles in the selective direction of small CDots toward subcellular organelles¹⁶. It was shown that blue-emitting CDots with neutral charge and –OH-based hybrid surface structures can preferentially penetrate the nuclear membrane, whereas green CDots with negative charge and carboxyl, carbonyl, or amide surface groups were excluded from the nucleus and instead localized to fibrous, network-like intracellular structures.

Potential artifacts. Artifacts caused by nanoparticle labeling have been frequently observed. The most commonly observed artifacts are aggregation and nonspecific binding. Some strategies have been developed to minimize these issues. For example, the introduction of small amounts of soluble PEG or a small percentage of fetal bovine serum into buffer solutions can minimize nonspecific absorption for PDots¹⁹ and CDots. Polyethylenimine is often introduced to improve the solubility and quantum yield of CDots; this approach has also been used to provide exposed amine groups for further conjugation to the morpholine group to target lysosomes⁴⁶. Bovine serum albumin at concentrations of 0.1% to 1% has been used broadly to improve the stability of nanoparticles and as a blocking agent to minimize nonspecific binding⁴⁷.

To test for artifacts in single-molecule tracking studies, researchers often use fluorescent proteins and dyes as positive controls, for example, to rule out the possible influence of the large size of nanoparticles on velocity or run length in typical single-nanoparticle tracking experiments^{23,25}. To exclude the nonspecific-binding

artifact, researchers typically carry out negative control experiments using nanoparticles without antibody⁴⁸. Fluorescent dyes are also useful for confirming the surface activity of nanoparticles before antibody conjugation. These types of controls are advisable for imaging with nanoparticles, especially those that are new or that target untested structures.

Future potential

Applications of luminescent nanoparticle probes in super-resolution microscopy are still in their infancy. As summarized in Table 1, there are many opportunities for these nanoparticle probes to be used in subcellular microscopy imaging, and a large scope for further developments.

Developing new modes of super-resolution imaging. This emerging field of research is characterized by its multidisciplinary and cross-disciplinary nature. The physics and photonics research communities have focused on exploring new ways to modulate the different optical properties of nanoparticles and developing new modes of super-resolution imaging (Fig. 3). The goal is to challenge records of resolution, contrast, and speed in recording super-resolution images of live cells with reduced phototoxicity.

With STED microscopy, the single-defect color centers in bulk diamond (Fig. 3a) can be imaged with a highest optical resolution of 2.4 nm and localization precision of 0.09 nm⁴⁹. Using the long-lived dark state of FNDs, Han et al. demonstrated a resolution of 12 nm with only a 16-mW (12 MW cm⁻²) laser in a ground-state-depletion

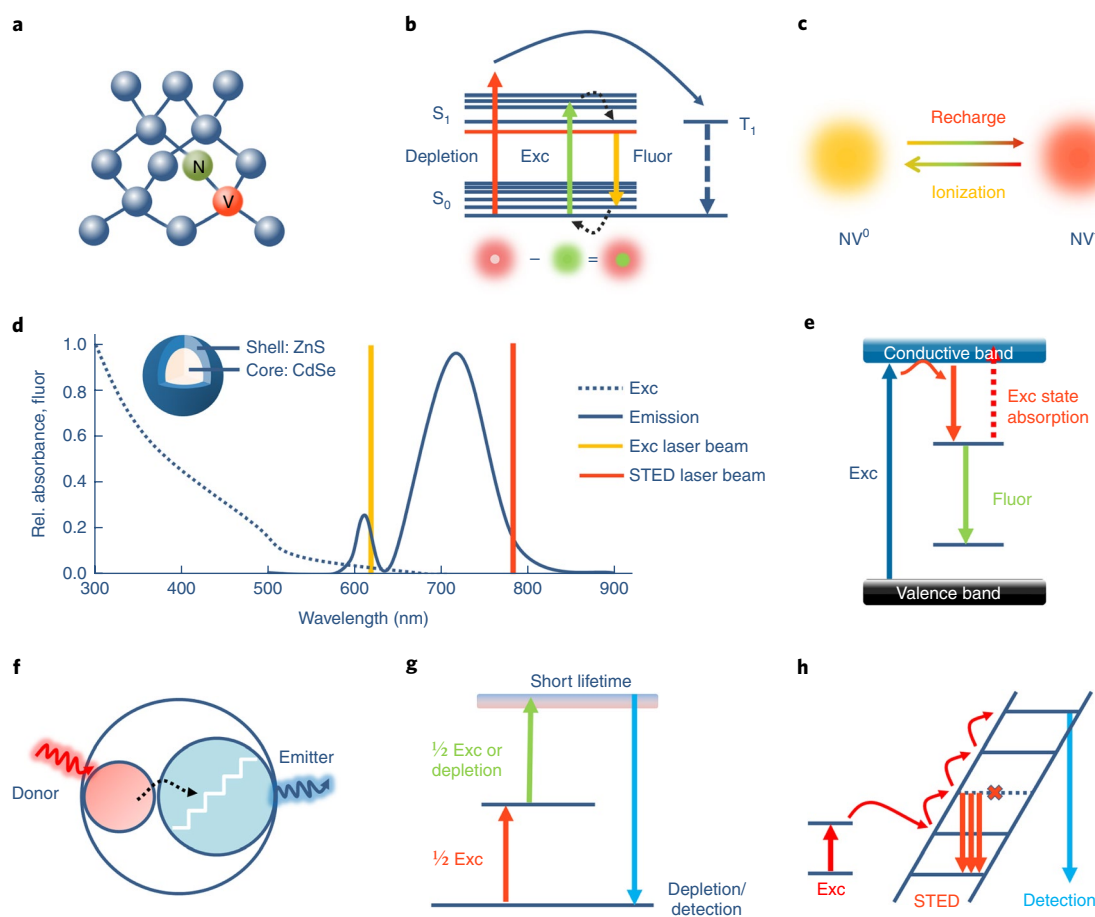


Fig. 3 | Typical schemes used to optically switch luminescent nanoparticles between their 'on' and 'off' states in super-resolution microscopy.

a, Schematic structure of the NV^- emitting center (N, nitrogen; V, vacancy) in FNDs. **b**, The photostability of FNDs in the triplet state allows a three-energy-level system to be formed so that ground-state depletion can be used to facilitate super-resolution⁵⁰. **c**, Through the conversion between NV^0 and NV^- states, charge-state depletion can also achieve super-resolution at low power⁵¹. **d**, The structure and the excitation and emission spectra of far-red-emitting QDs used in STED super-resolution microscopy^{2,3}. Rel., relative. **e**, The mechanism of excitation absorption in Mn-doped QDs used for super-resolution microscopy⁸⁵. **f**, Illustration of rare-earth-doped UCNPs containing highly doped Tm^{3+} emitters, suitable for STED microscopy. **g**, The 'ground'-state depletion of Pr^{3+} -doped UCNPs⁸⁶, in which the depletion and emission are of the same wavelength and, therefore, the detection has to be temporally separated. **h**, The ladder-like energy levels of the UCNPs and cross-relaxation between highly doped Tm^{3+} emitters can facilitate population inversion in the long-lifetime intermediate state, so that low depletion power is sufficient to modulate the upconverted blue emission¹². Exc, excitation; fluor, fluorescence.

process⁵⁰ (Fig. 3b). With a photochemical conversion scheme of ionization charge-state depletion (Fig. 3c), a low-power (48 mW or $\sim 27.7 \text{ MW cm}^{-2}$, assuming the 532-nm donut size of $1.734 \times 10^{-9} \text{ cm}^2$) laser achieves a 'negative-contrast' image with a resolution of 4.1 nm^5 . FNDs can be a versatile label for multimodal super-resolution imaging, such as STED microscopy⁵², structured illumination microscopy (SIM)⁵³, or localization-based super-resolution microscopy⁵⁴. Nevertheless, to the best of our knowledge, there has not been a successful report of efficient subcellular specific labeling using FNDs, largely because of their size ($>30 \text{ nm}$) and the associated issue of nonspecific labeling.

The intermittent-blinking behavior of QDs has enabled the physical science community to develop a variety of blinking-based statistical super-resolution techniques^{4,55–57}, particularly in Bayesian analysis of blinking and bleaching (3B), where an image resolution of 45 nm has been achieved². From a practical point of view and according to Table 1, for biological researchers considering nanoparticles for super-resolution, QDs have undergone the most development in terms of their commercial availability, small size, biocompatible surface, and compatibility with existing microscopy instruments, and should be the first choice for

microscopists aiming to test nanoparticles for intracellular imaging applications.

Finally, nanoparticles can be used for super-resolution functional imaging; for example, nonluminescent SERS nanoparticles have been used for super-resolution microscopy⁵⁸, to enhance the weak Raman signal and probe the vibrational 'fingerprint' of localized biological macromolecules. SERS spectroscopic characterization of single SERS nanoparticles, with movement tracking, has been shown to be useful as a reporter for the local molecular environment inside the living cell⁵⁹.

Integrating super-resolution microscopy and single-molecule tracking. The combination of super-resolution microscopy with single-molecule tracking presents an array of opportunities for interdisciplinary collaborations. The summary of the relationship between super-resolution microscopy and single-molecule tracking shown in Fig. 4 clearly illustrates the recent trend of combining ideas from different modalities. Because the field is rapidly evolving, clever combinations of different imaging modalities may provide synergistic effects that lead to improved imaging resolution, speed, and throughput. The combination of STED and SIM will generate

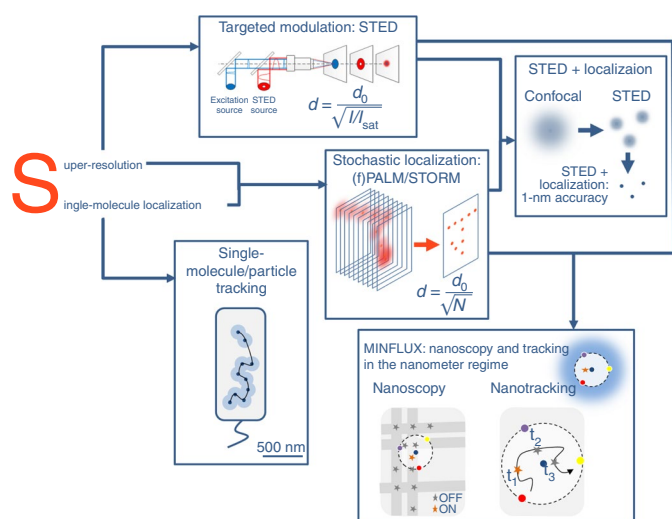


Fig. 4 | The evolution of super-resolution microscopy and single-molecule/particle localization approaches. Super-resolution approaches can be categorized as targeted modulation or stochastic localization; single-molecule localization is also widely applied in single-molecule/particle tracking. Combinations of these methods become powerful tools for determining the location of single particles, in order to study the dynamics of the nanoparticle and its tagged biomolecule(s). Colored dots in the MINFLUX panel (lower right) represent MINFLUX donut centers.

large-field-of-view and high-speed super-resolution images⁶⁰; combining SIM with nonlinear modulation yields nonlinear SIM to boost spatial resolution⁶¹; combination of the doughnut modulation in STED, interference pattern in SIM, and nonlinear modulation achieves both high resolution and a large field of view (high throughput) simultaneously⁶²; and STED can be used to introduce sparsity and improve the resolution of polarization-modulation-based modalities^{63,64}. New probes, being highly photostable and easily photoswitchable by lower-power excitation light, are in high demand, and could make multi-modal super-resolution microscopy widely accessible in the future.

New nanoparticles, in particular hybrid nanoparticle probes, will play an important role in this technology integration. Combined use of two dominant modulation mechanisms—for example, physically/optically structured modulation and stochastic photochemical modulation—has already led to substantial improvement in super-resolution. For example, once single NV⁻ centers (where N is nitrogen and V indicates vacancy) are resolved by STED imaging, a colocalization technique can be used to resolve a single NV⁻ center with a spatial-resolution accuracy of 1 Å⁶⁵. A super-resolution modality can also improve the accuracy of single-molecule tracking. For example, the recent successful development of MINFLUX⁶⁶, which uses a donut-shaped beam for excitation, has provided 1-nm accuracy in single-particle tracking and improved super-resolution imaging of small structures down to 1 nm. This suggests new opportunities in correlative super-resolution imaging and localization of single nanoparticles for dynamic imaging with responsive nanoparticle sensors⁵⁹. Furthermore, nanoparticles, as electron-dense materials, are expected to have considerable potential for correlated super-resolution light and electron microscopy.

Multi-‘color’ super-resolution imaging. The advent of genomic and proteomic approaches has opened a window on the various transcriptional and translational networks needed to sustain cellular functioning. An important next step is the visualization of these networks, at the single-molecule level, inside living cells. Although researchers have been able to visualize the dynamics of

transcription and translation inside cells at the single-molecule level^{67,68}, the development of tools that allow the visualization of such dynamics for many genes, transcripts, or proteins simultaneously is still in its infancy. Recently, several groups have developed barcoding methods to image transcripts in a highly multiplexed fashion^{69,70} via ingenious combinations of dye molecules.

Luminescent nanoparticles offer new opportunities to overcome spectral crowding by providing optical signatures along new dimensions through the use of luminescence lifetime, polarization, and a specific response to excitation intensity and pulse duration, all potentially extending the multiplexing capacity for super-resolution and making optical barcoding possible^{71–73}. Furthermore, design and controlled synthesis of nanoparticles with different sizes, shapes, compositions, or other aspects such as core-shell geometry and with integrated multifunctionality will offer more opportunities for multiplexing in super-resolution functional imaging⁷⁴.

Imaging bacterial systems. With the emergence of antimicrobial resistance as one of the greatest health challenges faced by modern society⁷⁵, there is a rapidly growing need for methods and imaging modalities that allow the study of molecular mechanisms in microbial systems, particularly bacteria. The much smaller size of bacterial systems compared with that of mammalian cells (typically a few micrometers compared with several tens to hundreds of micrometers) places different demands on imaging approaches. Although it is easier to rapidly visualize entire microbial cells within the field of view because of their very small size, there is a greater need for spatial resolution to enable the study of molecular processes based on subcellular spatiotemporal dynamics and localization. An additional challenge is the absence of uptake pathways that would allow the introduction of relatively large nanoparticle probes to the bacterial intracellular environment. Recent developments in electroporation methods suggest a viable approach to introduce high-molecular-weight particles into bacteria⁷⁶.

Single-molecule biosensing and diagnostics. The ability to discern binding events, biochemical reactions, or conformational changes at the single-molecule level in reconstituted systems based on purified proteins has greatly improved the overall understanding of molecular mechanisms⁷⁷. It has also created possibilities for ultrasensitive sensing applications in clinical, environmental, and biosecurity settings⁷⁸. However, biosensing approaches that rely on fluorescence as a readout are all hindered by low signals and limited photostability. Nanoparticles offer a favorable compromise between small fluorophores and large beads for single-molecule experiments in living cells, and are invaluable tools for ultrasensitive studies of the dynamics of cellular processes. Integration of bright and photostable nanoparticles with recently developed approaches that rely on single-molecule detection in sensitive, portable, and integrated microfluidics and other lab-on-a-chip platforms is needed to allow these methods to find wide use in practical settings.

Received: 27 July 2017; Accepted: 16 April 2018;
Published online: 28 May 2018

References

- Resch-Genger, U., Grabolle, M., Cavaliere-Jaricot, S., Nitschke, R. & Nann, T. Quantum dots versus organic dyes as fluorescent labels. *Nat. Methods* **5**, 763–775 (2008).
 - Yang, X. et al. Versatile application of fluorescent quantum dot labels in super-resolution fluorescence microscopy. *ACS Photonics* **3**, 1611–1618 (2016).
- This paper provides an overview of practical examples of the use of commercial quantum dots in a variety of super-resolution microscopy systems widely accessible to biological labs.**

3. Hanne, J. et al. STED nanoscopy with fluorescent quantum dots. *Nat. Commun.* **6**, 7127 (2015).
4. Dertinger, T., Colyer, R., Iyer, G., Weiss, S. & Enderlein, J. Fast, background-free, 3D super-resolution optical fluctuation imaging (SOFI). *Proc. Natl. Acad. Sci. USA* **106**, 22287–22292 (2009).
This paper reports a high-contrast super-resolution method (SOFI) for imaging quantum-dot-labeled microtubules of fibroblast cells.
5. Zeng, Z. et al. Fast super-resolution imaging with ultra-high labeling density achieved by joint tagging super-resolution optical fluctuation imaging. *Sci. Rep.* **5**, 8359 (2015).
6. Chen, X., Zeng, Z., Wang, H. & Xi, P. Three dimensional multimodal sub-diffraction imaging with spinning-disk confocal microscopy using blinking/fluctuation probes. *Nano Res.* **8**, 2251–2260 (2015).
7. Zhou, B., Shi, B., Jin, D. & Liu, X. Controlling upconversion nanocrystals for emerging applications. *Nat. Nanotechnol.* **10**, 924–936 (2015).
8. Fan, W., Bu, W. & Shi, J. On the latest three-stage development of nanomedicines based on upconversion nanoparticles. *Adv. Mater.* **28**, 3977–4011 (2016).
9. Chen, G., Qiu, H., Prasad, P. N. & Chen, X. Upconversion nanoparticles: design, nanochemistry, and applications in theranostics. *Chem. Rev.* **114**, 5161–5214 (2014).
10. Zhao, J. et al. Single-nanocrystal sensitivity achieved by enhanced upconversion luminescence. *Nat. Nanotechnol.* **8**, 729–734 (2013).
11. Gargas, D. J. et al. Engineering bright sub-10-nm upconverting nanocrystals for single-molecule imaging. *Nat. Nanotechnol.* **9**, 300–305 (2014).
12. Liu, Y. et al. Amplified stimulated emission in upconversion nanoparticles for super-resolution nanoscopy. *Nature* **543**, 229–233 (2017).
This paper describes highly doped upconversion nanoparticles suitable for low-power, high-contrast super-resolution microscopy with optical resolution 1/36 of the excitation wavelength.
13. Zhan, Q. et al. Achieving high-efficiency emission depletion nanoscopy by employing cross relaxation in upconversion nanoparticles. *Nat. Commun.* **8**, 1058 (2017).
14. Wang, B. et al. A mitochondria-targeted fluorescent probe based on TPP-conjugated carbon dots for both one- and two-photon fluorescence cell imaging. *RSC Advances* **4**, 49960–49963 (2014).
15. Leménager, G., De Luca, E., Sun, Y.-P. & Pompa, P. P. Super-resolution fluorescence imaging of biocompatible carbon dots. *Nanoscale* **6**, 8617–8623 (2014).
This paper reports STED super-resolution microscopy using biocompatible CDots in both fixed and living cells.
16. Chizhik, A. M. et al. Super-resolution optical fluctuation bio-imaging with dual-color carbon nanodots. *Nano Lett.* **16**, 237–242 (2016).
17. Khan, S., Verma, N. C., Gupta, A. & Nandi, C. K. Reversible photoswitching of carbon dots. *Sci. Rep.* **5**, 11423 (2015).
18. He, H. et al. High-density super-resolution localization imaging with blinking carbon dots. *Anal. Chem.* **89**, 11831–11838 (2017).
This paper systematically compares the performance of CDots and Cy3, Cy5, Alexa Fluor 647, and QDots 605, and shows that the stable blinking of CDots is suitable for high-density localization imaging of microtubules and membrane protein receptors.
19. Wu, C. et al. Bioconjugation of ultrabright semiconducting polymer dots for specific cellular targeting. *J. Am. Chem. Soc.* **132**, 15410–15417 (2010).
This paper reports surface-functionalized polymer dots for covalent conjugation to biomolecules, and systematically validates the exceptional brightness of polymer dots compared with that of Alexa Fluor dyes and quantum dot probes.
20. Chen, X. et al. Small photoblinking semiconductor polymer dots for fluorescence nanoscopy. *Adv. Mater.* **29**, 1604850 (2017).
21. Fang, X. et al. Multicolor photo-crosslinkable AIEgens toward compact nanodots for subcellular imaging and STED nanoscopy. *Small* **13**, 1702128 (2017).
22. Li, D., Qin, W., Xu, B., Qian, J. & Tang, B. Z. AIE nanoparticles with high stimulated emission depletion efficiency and photobleaching resistance for long-term super-resolution bioimaging. *Adv. Mater.* **29**, 1703643 (2017).
23. Dahan, M. et al. Diffusion dynamics of glycine receptors revealed by single-quantum dot tracking. *Science* **302**, 442–445 (2003).
24. Lowe, A. R. et al. Selectivity mechanism of the nuclear pore complex characterized by single cargo tracking. *Nature* **467**, 600–603 (2010).
This paper systematically studies how the nuclear pore complex facilitates the translocation of transport cargo complexes by tracking a large number of single protein-functionalized quantum dots.
25. Cui, B. et al. One at a time, live tracking of NGF axonal transport using quantum dots. *Proc. Natl. Acad. Sci. USA* **104**, 13666–13671 (2007).
26. Chowdary, P. D. et al. Nanoparticle-assisted optical tethering of endosomes reveals the cooperative function of dyneins in retrograde axonal transport. *Sci. Rep.* **5**, 18059 (2015).
27. Warshaw, D. M. et al. Differential labeling of myosin V heads with quantum dots allows direct visualization of hand-over-hand processivity. *Biophys. J.* **88**, L30–L32 (2005).
28. Yu, J. et al. Nanoscale 3D tracking with conjugated polymer nanoparticles. *J. Am. Chem. Soc.* **131**, 18410–18414 (2009).
29. Chang, Y.-R. et al. Mass production and dynamic imaging of fluorescent nanodiamonds. *Nat. Nanotechnol.* **3**, 284–288 (2008).
30. Haziza, S. et al. Fluorescent nanodiamond tracking reveals intraneuronal transport abnormalities induced by brain-disease-related genetic risk factors. *Nat. Nanotechnol.* **12**, 322–328 (2017).
31. Tzeng, Y. K. et al. Superresolution imaging of albumin-conjugated fluorescent nanodiamonds in cells by stimulated emission depletion. *Angew. Chem. Int. Ed. Engl.* **50**, 2262–2265 (2011).
This paper demonstrates STED super-resolution imaging of single photostable fluorescent nanodiamonds in cells.
32. Bae, Y. M. et al. Endocytosis, intracellular transport, and exocytosis of lanthanide-doped upconverting nanoparticles in single living cells. *Biomaterials* **33**, 9080–9086 (2012).
33. Nam, S. H. et al. Long-term real-time tracking of lanthanide ion doped upconverting nanoparticles in living cells. *Angew. Chem.* **123**, 6217–6221 (2011).
This paper reports real-time tracking of near-infrared excited photostable upconverting nanoparticles in living cells for as long as 6 h.
34. Jo, H. L. et al. Fast and background-free three-dimensional (3D) live-cell imaging with lanthanide-doped upconverting nanoparticles. *Nanoscale* **7**, 19397–19402 (2015).
35. Liu, M. et al. Real-time visualization of clustering and intracellular transport of gold nanoparticles by correlative imaging. *Nat. Commun.* **8**, 15646 (2017).
36. Tracking nanoparticles by eye. *Nat. Methods* **15**, 164 (2018).
37. Wang, F. et al. Microscopic inspection and tracking of single upconversion nanoparticles in living cells. *Light Sci. Appl.* **7**, 18007 (2018).
This paper shows that single upconversion nanoparticles are very bright, stable and bleach resistant, and can be detected within cells by eye through the microscope eyepiece, thus providing a new tool for tracking experiments.
38. Sedlmeier, A. & Gorris, H. H. Surface modification and characterization of photon-upconverting nanoparticles for bioanalytical applications. *Chem. Soc. Rev.* **44**, 1526–1560 (2015).
39. Wegner, K. D. & Hildebrandt, N. Quantum dots: bright and versatile in vitro and in vivo fluorescence imaging biosensors. *Chem. Soc. Rev.* **44**, 4792–4834 (2015).
40. Derfus, A. M., Chan, W. C. & Bhatia, S. N. Intracellular delivery of quantum dots for live cell labeling and organelle tracking. *Adv. Mater.* **16**, 961–966 (2004).
41. Delehanty, J. B., Mattoussi, H. & Medintz, I. L. Delivering quantum dots into cells: strategies, progress and remaining issues. *Anal. Bioanal. Chem.* **393**, 1091–1105 (2009).
42. Courty, S., Luccardini, C., Bellaiche, Y., Cappello, G. & Dahan, M. Tracking individual kinesin motors in living cells using single quantum-dot imaging. *Nano Lett.* **6**, 1491–1495 (2006).
43. Sun, Y. et al. A supramolecular self-assembly strategy for upconversion nanoparticle bioconjugation. *Chem. Commun. (Camb.)* **54**, 3851–3854 (2018).
44. Drees, C. et al. Engineered upconversion nanoparticles for resolving protein interactions inside living cells. *Angew. Chem. Int. Ed. Engl.* **55**, 11668–11672 (2016).
45. Jung, Y. K., Shin, E. & Kim, B.-S. Cell nucleus-targeting zwitterionic carbon dots. *Sci. Rep.* **5**, 18807 (2015).
46. Wu, L., Li, X., Ling, Y., Huang, C. & Jia, N. Morpholine derivative-functionalized carbon dots-based fluorescent probe for highly selective lysosomal imaging in living cells. *ACS Appl. Mater. Interfaces* **9**, 28222–28232 (2017).
47. Pinaud, F., King, D., Moore, H.-P. & Weiss, S. Bioactivation and cell targeting of semiconductor CdSe/ZnS nanocrystals with phytochelatin-related peptides. *J. Am. Chem. Soc.* **126**, 6115–6123 (2004).
48. Navas-Moreno, M. et al. Nanoparticles for live cell microscopy: a surface-enhanced Raman scattering perspective. *Sci. Rep.* **7**, 4471 (2017).
49. Wildanger, D. et al. Solid immersion facilitates fluorescence microscopy with nanometer resolution and sub-ångström emitter localization. *Adv. Mater.* **24**, OP309–OP313 (2012).
50. Han, K. Y., Kim, S. K., Eggeling, C. & Hell, S. W. Metastable dark states enable ground state depletion microscopy of nitrogen vacancy centers in diamond with diffraction-unlimited resolution. *Nano Lett.* **10**, 3199–3203 (2010).
51. Chen, X. et al. Subdiffraction optical manipulation of the charge state of nitrogen vacancy center in diamond. *Light Sci. Appl.* **4**, e230 (2015).
52. Han, K. Y. et al. Three-dimensional stimulated emission depletion microscopy of nitrogen-vacancy centers in diamond using continuous-wave light. *Nano Lett.* **9**, 3323–3329 (2009).
53. Yang, X. et al. Sub-diffraction imaging of nitrogen-vacancy centers in diamond by stimulated emission depletion and structured illumination. *RSC Advances* **4**, 11305–11310 (2014).

54. Chen, E. H., Gaathon, O., Trusheim, M. E. & Englund, D. Wide-field multispectral super-resolution imaging using spin-dependent fluorescence in nanodiamonds. *Nano Lett.* **13**, 2073–2077 (2013).
55. Yahiatene, I., Hennig, S., Müller, M. & Huser, T. Entropy-based super-resolution imaging (ESI): from disorder to fine detail. *ACS Photonics* **2**, 1049–1056 (2015).
56. Mandula, O., Šestak, I. Š., Heintzmann, R. & Williams, C. K. Localisation microscopy with quantum dots using non-negative matrix factorisation. *Opt. Express* **22**, 24594–24605 (2014).
57. Cox, S. et al. Bayesian localization microscopy reveals nanoscale podosome dynamics. *Nat. Methods* **9**, 195–200 (2011).
58. Hennig, S., Mönkemöller, V., Böger, C., Müller, M. & Huser, T. Nanoparticles as nonfluorescent analogues of fluorophores for optical nanoscopy. *ACS Nano* **9**, 6196–6205 (2015).
59. Ando, J., Fujita, K., Smith, N. I. & Kawata, S. Dynamic SERS imaging of cellular transport pathways with endocytosed gold nanoparticles. *Nano Lett.* **11**, 5344–5348 (2011).
60. Yang, B., Przybilla, F., Mestre, M., Trebbia, J.-B. & Lounis, B. Large parallelization of STED nanoscopy using optical lattices. *Opt. Express* **22**, 5581–5589 (2014).
61. Rego, E. H. et al. Nonlinear structured-illumination microscopy with a photoswitchable protein reveals cellular structures at 50-nm resolution. *Proc. Natl. Acad. Sci. USA* **109**, E135–E143 (2012).
62. Chmyrov, A. et al. Nanoscopy with more than 100,000 ‘doughnuts’. *Nat. Methods* **10**, 737–740 (2013).
63. Zhanghao, K. et al. Super-resolution with dipole orientation mapping via polarization demodulation. *Light Sci. Appl.* **5**, e16166 (2016).
64. Hafi, N. et al. Fluorescence nanoscopy by polarization modulation and polarization angle narrowing. *Nat. Methods* **11**, 579–584 (2014).
65. Rittweger, E., Han, K., Irvine, S., Eggeling, C. & Hell, S. STED microscopy reveals crystal colour centres with nanometric resolution. *Nat. Photonics* **3**, 144–147 (2009).
66. Balzarotti, F. et al. Nanometer resolution imaging and tracking of fluorescent molecules with minimal photon fluxes. *Science* **355**, 606–612 (2017).
67. Yu, J., Xiao, J., Ren, X., Lao, K. & Xie, X. S. Probing gene expression in live cells, one protein molecule at a time. *Science* **311**, 1600–1603 (2006).
68. Park, H. Y. et al. Visualization of dynamics of single endogenous mRNA labeled in live mouse. *Science* **343**, 422–424 (2014).
69. Lubeck, E. & Cai, L. Single-cell systems biology by super-resolution imaging and combinatorial labeling. *Nat. Methods* **9**, 743–748 (2012).
70. Chen, K. H., Boettiger, A. N., Moffitt, J. R., Wang, S. & Zhuang, X. Spatially resolved, highly multiplexed RNA profiling in single cells. *Science* **348**, aaa6090 (2015).
71. Lu, Y. et al. Tunable lifetime multiplexing using luminescent nanocrystals. *Nat. Photonics* **8**, 32–36 (2014).
72. Dong, H. et al. Versatile spectral and lifetime multiplexing nanoplatform with excitation orthogonalized upconversion luminescence. *ACS Nano* **11**, 3289–3297 (2017).
73. Lin, G., Baker, M. A. B., Hong, M. & Jin, D. The quest for optical multiplexing in bio-discoveries. *Chem* **4**, 997–1021 (2018).
74. Liu, D. et al. Three-dimensional controlled growth of monodisperse sub-50 nm heterogeneous nanocrystals. *Nat. Commun.* **7**, 10254 (2016).
75. O'Neill, J. *Rapid Diagnostics: Stopping Unnecessary Use of Antibiotics* (Review on Antimicrobial Resistance, London, 2015).
76. Plochowitz, A., Crawford, R. & Kapanidis, A. N. Characterization of organic fluorophores for in vivo FRET studies based on electroporated molecules. *Phys. Chem. Chem. Phys.* **16**, 12688–12694 (2014).
77. van Oijen, A. M. & Dixon, N. E. Probing molecular choreography through single-molecule biochemistry. *Nat. Struct. Mol. Biol.* **22**, 948–952 (2015).
78. Gooding, J. J. & Gaus, K. Single-molecule sensors: challenges and opportunities for quantitative analysis. *Angew. Chem. Int. Ed. Engl.* **55**, 11354–11366 (2016).
79. Hoyer, P., Staudt, T., Engelhardt, J. & Hell, S. W. Quantum dot blueing and blinking enables fluorescence nanoscopy. *Nano Lett.* **11**, 245–250 (2011).
80. Xu, J., Tehrani, K. F. & Kner, P. Multicolor 3D super-resolution imaging by quantum dot stochastic optical reconstruction microscopy. *ACS Nano* **9**, 2917–2925 (2015).
81. Chen, X. et al. Multicolor super-resolution fluorescence microscopy with blue and carmine small photoblinking polymer dots. *ACS Nano* **11**, 8084–8091 (2017).
82. McGuinness, L. P. et al. Quantum measurement and orientation tracking of fluorescent nanodiamonds inside living cells. *Nat. Nanotechnol.* **6**, 358–363 (2011).
83. Leduc, C. et al. A highly specific gold nanoprobe for live-cell single-molecule imaging. *Nano Lett.* **13**, 1489–1494 (2013).
84. Wu, C. et al. Ultrabright and bioorthogonal labeling of cellular targets using semiconducting polymer dots and click chemistry. *Angew. Chem. Int. Ed. Engl.* **49**, 9436–9440 (2010).
85. Irvine, S. E., Staudt, T., Rittweger, E., Engelhardt, J. & Hell, S. W. Direct light-driven modulation of luminescence from Mn-doped ZnSe quantum dots. *Angew. Chem. Int. Ed. Engl.* **47**, 2685–2688 (2008).
86. Kolesov, R. et al. Super-resolution upconversion microscopy of praseodymium-doped yttrium aluminum garnet nanoparticles. *Phys. Rev. B* **84**, 153413 (2011).
87. Cutler, P. J. et al. Multi-color quantum dot tracking using a high-speed hyperspectral line-scanning microscope. *PLoS One* **8**, e64320 (2013).
88. Keller, A. M. et al. 3-dimensional tracking of non-blinking ‘giant’ quantum dots in live cells. *Adv. Funct. Mater.* **24**, 4796–4803 (2014).
89. Hatakeyama, H., Nakahata, Y., Yarimizu, H. & Kanzaki, M. Live-cell single-molecule labeling and analysis of myosin motors with quantum dots. *Mol. Biol. Cell* **28**, 173–181 (2017).

Acknowledgements

The authors acknowledge S. Qu (Changchun Institute of Optics Fine Mechanics and Physics, Chinese Academy of Sciences), C. Wu (Southern University of Science and Technology), Q. Su, O. Shimoni, and F. Wang for valuable technical discussions. D.J., A.M.v.O., and P.X. acknowledge support from the Australian Research Council (FT 130100517, FL140100027) and the National Natural Science Foundation of China (61729501, 51720105015). J.E. is grateful for financial support from the Cluster of Excellence and DFG Research Centre Nanoscale Microscopy and Molecular Physiology of the Brain (CNMPB).

Competing interests

The authors declare no competing interests.

Additional information

Reprints and permissions information is available at www.nature.com/reprints.

Correspondence should be addressed to D.J. or P.X. or J.E. or A.M.v.O.

Publisher's note: Springer Nature remains neutral with regard to jurisdictional claims in published maps and institutional affiliations.